Molecular Biology of the Cell
Vol. 17, 1218–1227, March 2006

Distinct Ceramide Synthases Regulate Polarized Growth in the Filamentous Fungus *Aspergillus nidulans*[D]

Shaojie Li,* Liangcheng Du,† Gary Yuen,* and Steven D. Harris*‡

Departments of *Plant Pathology and †Chemistry and ‡Plant Science Initiative, University of Nebraska, Lincoln, NE 68588-0660

Submitted June 14, 2005; Revised December 8, 2005; Accepted December 27, 2005
Monitoring Editor: Howard Riezman

In filamentous fungi, the stabilization of a polarity axis is likely to be a pivotal event underlying the emergence of a germ tube from a germinating spore. Recent results implicate the polarisome in this process and also suggest that it requires localized membrane organization. Here, we employ a chemical genetic approach to demonstrate that ceramide synthesis is necessary for the formation of a stable polarity axis in the model fungus *Aspergillus nidulans*. We demonstrate that a novel compound (HSAF) produced by a bacterial biocontrol agent disrupts polarized growth and leads to loss of membrane organization and formin localization at hyphal tips. We show that BarA, a putative acyl-CoA-dependent ceramide synthase that is unique to filamentous fungi mediates the effects of HSAF. Moreover, *A. nidulans* possesses a second likely ceramide synthase that is essential and also regulates hyphal morphogenesis. Our results suggest that filamentous fungi possess distinct pools of ceramide that make independent contributions to polarized hyphal growth, perhaps through the formation of specialized lipid microdomains that regulate organization of the cytoskeleton.

INTRODUCTION

Polarized hyphal growth is the defining feature of filamentous fungi. Fungal hyphae grow by apical extension (Bartnicki-Garcia and Lippman, 1969; Gooday, 1971), whereby vesicles containing precursors required for cell wall deposition and cell surface expansion are delivered to a discrete region at the hyphal tip. Vesicles initially undergo long-range transport from the interior to the tip region along polarized arrays of cytoplasmic microtubules. At the tip, they aggregate as a complex termed the Spitzenkorper (Bartnicki-Garcia, 2002), which mediates the localized dispersal of vesicles to their ultimate destination. This final transport step utilizes the actin cytoskeleton. The molecular mechanisms underlying polarized hyphal growth are being characterized with increasing detail (Harris and Momany, 2004; Harris *et al.*, 2005). These efforts reveal a complex process that appears to share features in common with other highly polarized cells, such as neurons.

The formins are actin filament-nucleating proteins involved in polarized growth and related processes in animals, plants, and fungi (Higgs and Peterson, 2005). Like most filamentous fungi, *Aspergillus nidulans* possesses a single formin, SepA. Previous studies show that SepA is required for the formation of a stable axis of polarized hyphal growth and for septum formation (Harris *et al.*, 1997). SepA exhibits a dynamic localization pattern at hyphal tips and septation sites (Sharpless and Harris, 2002), which suggests that its recruitment to these sites is highly regulated. Candidate regulators include conserved components of the polarisome, such as Spa2 and Bud6 (Sheu *et al.*, 1998; Sagot *et al.*, 2002). In addition, recent results implicate localized membrane organization as being an important determinant of SepA recruitment (Pearson *et al.*, 2004). Notably, sphingolipids are required for SepA localization to the hyphal tip (Pearson *et al.*, 2004), which may account for their essential role in the polarized growth of *A. nidulans* hyphae (Cheng *et al.*, 2001).

Sphingolipids are components of specialized membrane microdomains that are thought to play key roles in cell signaling and cytoskeletal organization (Futerman and Hannun, 2004). The biologically active molecule ceramide is a simplified sphingolipid that is synthesized by the condensation of a fatty acyl-CoA with a sphingoid base (Merrill, 2002). The responsible enzyme, acyl CoA-dependent ceramide synthase, can utilize acyl chains of varying lengths, though the well-characterized yeast enzyme prefers C26 fatty acyl-CoA as the substrate (Guillas *et al.*, 2001). In *Saccharomyces cerevisiae*, Lag1 and Lac1 are homologous ceramide synthases that generate the bulk of ceramide pools (Guillas *et al.*, 2001; Schorling *et al.*, 2001). The remainder is produced via reverse ceramidase activity (Schorling *et al.*, 2001). Deletion of either *LAG1* or *LAC1* does not cause obvious growth defects; however, the double *lag1 lac1* mutant is severely crippled and displays cell wall defects (Barz and Walter, 1999; Schorling *et al.*, 2001). Recent biochemical characterization of Lag1 and Lac1 resulted in the identification of an additional subunit, Lip1, which is required for ceramide synthase activity (Vallee and Riezman, 2005).

The bacterial biocontrol agent *Lysobacter enzymogenes* C3 exhibits promising plant protection activity against fungal plant pathogens (Zhang and Yuen, 1999; Yuen *et al.*, 2001). A component of this activity is a heat-stable antifungal factor (HSAF). We have found that HSAF dramatically affects the polarized growth of *A. nidulans* hyphae. These effects include the rapid loss of SepA localization from growing hyphal tips. The characterization of mutants displaying al-

This article was published online ahead of print in *MBC in Press* (http://www.molbiolcell.org/cgi/doi/10.1091/mbc.E05–06–0533) on January 4, 2006.

[D] The online version of this article contains supplemental material at *MBC Online* (http://www.molbiolcell.org).

Address correspondence to: Steven D. Harris (sharri1@unlnotes.unl.edu).

Table 1. Strain list

Strain	Relevant phenotype	Source
A28	*pabaA6 biA1*	FGSC[a]
GR5	*pyrG89; wA3*	FGSC[a]
UV13	*barA1; pabaA6 biA1*	This study
UV2	*barA2; pabaA6 biA1*	This study
UV20	*barA3; pabaA6 biA1*	This study
UV1	*barA4; pabaA6 biA1*	This study
8-145	*basA1; pabaA6 biA1*	This study
ACP115	*tpmA::GFP::pyr-4; pyrG89; wA3*	Pearson *et al.* (2004)
AKS70	*sepA::gfp::pyr-4; pyrG89 pabaA1 yA2*	Sharpless and Harris (2002)
RCP12	*barA1; tpmA::GFP::pyr-4; pyrG89; wA3*	This study
SCP1	*basA1; tpmA::GFP::pyr-4; pyrG89; wA3*	This study
ASL10	*alcA*(p)::*GFP::lagA::pyr-4; pyrG89; wA3*	This study
DRG1	*alcA*(p)::*GFP::lagA::pyr-4; barA1; pyrG89; wA3*	This study
ASL11	Δ*lagA::pyr-4; pyrG89; wA3*	This study

[a] Fungal Genetic Stock Center, Department of Microbiology, University of Kansas Medical Center, Kansas City, KS 66160-7420.

tered responses to HSAF reveals that a ceramide synthesis pathway is required for its effects. Further molecular analyses demonstrate that *A. nidulans* possesses two distinct ceramide synthases that regulate hyphal morphogenesis: an essential Lag1 homologue and an additional enzyme unique to filamentous fungi that is required for the maintenance of a stable axis of hyphal polarity.

MATERIALS AND METHODS

Fungal Strains and Media

Strains used in this study are described in Table 1. Media used for growing *A. nidulans* include MN (1% glucose, nitrate salts, trace elements, pH 6.5), MN-VTF (0.1 M threonine, 0.1% fructose, nitrate salts, trace elements, and vitamins, pH 6.5), MAG (2% malt extract, 2% glucose, 0.2% peptone, trace elements, and vitamins), and YGV (2% dextrose, 0.5% yeast extracts, and vitamins). Trace elements, vitamins, and nitrate salts are described in the appendix to Kafer (1977). Media were solidified using 1.5% agar. Uridine (5 mM) and uracil (10 mM) were added as needed. Strains were grown at 28°C; for temperature sensitive (Ts) strains, permissive temperature was 28°C and restrictive temperature was 42°C.

Preparation of HSAF

HSAF was prepared from *Lysobacter enzymogenes* strain C3R5 (Zhang and Yuen, 1999) grown in 10% TSB liquid medium. Cell-free broth cultures were subject to ammonium sulfate precipitation followed by methanol extraction. HSAF was dissolved in methanol to produce a stock solution (20 mg/ml), which was stored at −20°C. Additional purification by HPLC yielded purified material that was subjected to NMR analysis and was shown to possess a structure related to a family of antibiotics containing maltophilin and dihydromaltophilin (L. Du *et al.*, unpublished results). HPLC-purified HSAF had the same activity as the partially purified material when tested in growth and morphological assays (Supplementary Figure 1). Because the amount of purified material was so small, the methanol extracts were used for most experiments.

Microscopy

Coverslips with adherent hyphae were prepared for microscopy as previously described (Harris *et al.*, 1994). Cell walls, nuclei, and sterol-rich membrane microdomains were detected as previously described using Calcofluor, Hoechst 33258, and filipin, respectively (Harris *et al.*, 1994; Pearson *et al.*, 2004). To visualize GFP fusion proteins, hyphae grown on coverslips in YGV were briefly rinsed in sterile water and mounted. SepA-GFP was detected in transformants possessing plasmid pKES59 (Sharpless and Harris, 2002). Microfilaments were visualized in transformants containing a tropomyosin GFP fusion (TpmA-GFP) on plasmid pCP32 (Pearson *et al.*, 2004). In all cases, GFP constructs were expressed under control of native promoter sequences. Microscopic observations were made using the 40× (UPlanApo) and 60× objectives (PlanApo) of an Olympus BX51 fluorescent microscope. Images were captured with a Photometrics CoolSnap HQ CCD camera (Roper Scientific, Tucson, AZ) and processed using IPLab software (Scanalytics, Billerica, MA). Images were converted from 16 to 8 bits and saved as TIF files. Additional processing was performed using Adobe PhotoShop 6.0 (San Jose, CA).

HSAF Susceptibility Tests and Mutant Screens

HSAF was added to autoclaved media. In some cases, Tergitol NP-40 (Sigma, St. Louis, MO) was added to a final concentration of 0.05% to improve solubility. Equivalent amounts of solvent were added to control plates. To generate HSAF-resistant mutants, conidiospores (strain A28) were plated onto MAG containing HSAF (50 μg/ml) and mutagenized with UV light (100J/m^2) at a kill rate of 90%. Plates were incubated at 28°C for 3 d and larger colonies selected for subsequent analysis. HSAF-hypersensitive mutants were recovered by screening a large collection of Ts mutants (Harris *et al.*, 1994) for those unable to form colonies at 28°C in MAG containing HSAF (50 μg/ml). Candidate mutants were further tested for HSAF-induced defects in polarized hyphal growth. Note that the mutants displayed equal levels of resistance (Supplementary Figure 1) or sensitivity to HPLC-purified HSAF. However, because the partially purified methanol-extracted material could be readily produced in sufficiently large amounts, it was used for most experiments.

Genetic Analysis of Mutants and Characterization of the Affected Genes

Standard approaches were used for mutant characterization (Harris, 2001). The affected genes were cloned by complementation using a genomic library constructed in the vector pRG3-AMA1 (Osherov and May, 2000; available from the Fungal Genetics Stock Center, Kansas City, MO). Protoplast preparation and transformation were performed as previously described (Oakley and Osmani, 1993). Complementation was judged by restoration of wild-type growth and morphology at restrictive temperature. Plasmid dependency was verified by evicting complementing plasmids on MN media containing 5-fluororotic acid (5-FOA) and testing for restoration of the original mutant phenotype (O'Connell *et al.*, 1992). Plasmids were recovered and transformed into *Escherichia coli* DH5α for amplification and then retested to confirm that they possess complementing activity.

Inserts were amplified from complementing plasmids using oligonucleotide primers that flank the cloning site. The sequence of ~500 nucleotides was determined for each end of the insert and compared with the *A. nidulans* genome sequence database (http://www.broad.mit.edu/annotation/fungi/fgi/) to identify its boundaries. Predicted open reading frames located on each insert were individually amplified and tested for complementation when cotransformed with pRG3-AMA1 (Efimov and Morris, 1998). Once identified as the affected gene, the coding region was independently amplified and sequenced in triplicate to verify the presence of a mutation and determine its nature.

The fusion PCR approach recently described by Yang *et al.* (2004) was used to replace *lagA* with *pyr-4*. Briefly, we amplified the 5′ flanking sequence (2031-base pairs) with primers Rlac1 (5′ATCTCCAGTAAATGCCGCCC) and Rlac2 (5′CCGCACAGATGCGTAAGGAGATTTGTCAAACCGTTCTCCCACTG), the 3′ flanking sequence with primers Rlac3 (5′CAGTACAATCTGCTCTGATGCATGGGTTTGTCCGCATTTTTCT) and Rlac4 (5′GGACAAGCCTCTCATTCTCG), and *pyr-4* with primers Rlac5 (5′GCAAATGACAGTGGGAGAACGGTTTGACAAATCTCCTTACGCATCTGTGCGG) and Rlac6 (5′AAGGGAAGAAGAGAAAAATGCGGACAAACCCATGCATCAGAGCAGATTGTTACTG). The amplified 5′ flank has 53-base pairs of sequence overlap at its 3′ end with the 5′ extension of the *pyr-4* product. The amplified 3′ flank has 54-base

pairs of sequence overlap at its 5′ end with the 3′ extension of the *pyr-4* product. The final gene replacement was generated using primers Rlac1 and Rlac4 with a template consisting of a mixture of the three amplified fragments (120 ng each). The fusion PCR was performed using programs specified by Yang *et al.* (2004). The final gene replacement was cloned into the TOPO vector (Invitrogen, Carlsbad, CA) to produce plasmid pLACR12. The *lagA* deletion mutant was subsequently generated by transformation of wild-type strain GR5 with pLACR12.

The conditional *lagA* allele, *alcA*(p)::*GFP*::*lagA*, was constructed in plasmid pMCB17apx (Efimov, 2003). A 761-base pair fragment starting from the predicted initiation codon of *lagA* was amplified with the primers ASC2464F (CATCGGCGCGGCCGATGGCTCGCACGCGCAAATCCA; *Asc*I site underlined) and Pac2464R (ACCTTAATTAAGCGAAGGAGAACAATAGCCTGCTGG; *Pac*I site underlined). The amplified fragment was cloned into pMCB17apx using the *Asc*I and *Pac*I cloning sites, thereby fusing the N-terminus of LagA to GFP, which in turn is expressed under the control of *alcA*(p). Homologous integration of this construct generates a single full-length copy of *lagA* regulated by *alcA*(p), plus a truncated version controlled by native promoter sequences. Accordingly, transformants are propagated under *alcA*(p) inducing conditions (1% glycerol), then shifted to repressing conditions (1% glucose) to observe mutant phenotypes (Oakley and Osmani, 1993).

Labeling and Analysis of Sphingolipids

Wild-type (GR5), *barA* mutant (UV13), *alcA*(p)::*GFP*::*lagA* (ASL10), and *alcA*(p)::*GFP*::*lagA barA* (DRG1) conidiospores were inoculated into 25 ml YGV (supplemented with uridine and uracil when necessary). After incubating at 28°C, 180 rpm for 2 d, mycelia were filtered through four layers of Miracloth. Approximately 100 mg (wet weight) of mycelia was transferred into a sterile 15-ml test tube containing 3 ml fresh YGV. Hyphae were allowed to grow overnight under the same conditions, and an aliquot of 200 μl was transferred to a new tube and grown for an additional 4 h. To label de novo synthesized sphingolipids, 5 μl of [4,5-[^{3}H]D-erythro-dihydrosphingosine (DHS; 60 Ci/mmol, 1 μCi/μl, American Radiolabeled Chemicals, St. Louis, MO) was added to the cultures. After shaking at 180 rpm for 1 h, 400 μl fresh YGV was added to the cultures and growth continued for an additional 4 h. Mycelia were harvested by centrifugation (3000 $\times$ *g*) and lipids extracted using 95% ethanol-water-diethylether-pyridine-ammonium hydroxide (15:15:5:1:0.018, vol/vol) as described previously (Cheng *et al.*, 2001; Schorling *et al.*, 2001). Lipid extracts were dried in a Speed-Vac and resuspended in a methanol-water-butanol-methylamine (4:3:1:5, vol/vol) for methanolysis. The solution was incubated at 52°C for 30 min to permit deacylation of lipids. The mixture was dried in a Speed-Vac and resuspended in chloroform-methanol-H_2O (16:16:5, vol/vol). Finally, the deacylated lipid mixtures were loaded to a TLC plate (Silica Gel 60, EM Merck) and separated using a solvent system of chloroform-methanol-4.2 N ammonium hydroxide (9:7:2, vol/vol). The ^{3}H-labeled metabolites were visualized by autoradiography using Hyperfilm ECL (Amersham Biosciences, Amersham, Buckinghamshire, United Kingdom).

RESULTS

HSAF Affects Polarized Hyphal Growth

HSAF is a low-molecular-weight (i.e., 512 Da) polyketide that initially drew interest because it exhibits antifungal activity against a number of plant pathogenic fungi (Li, 2005). Preliminary structural analysis revealed that HSAF is related to a known family of antibiotics containing maltophilin and dihydromaltophilin (Jakobi *et al.*, 1996; Graupner *et al.*, 1997; L. Du *et al.*, unpublished results). Although HSAF is active against a broad range of fungi, including ascomycetes and basidiomycetes, it has negligible effects on the growth of *S. cerevisiae*. Therefore, as a first step toward determining its mode of action, we tested the effect of partially purified HSAF (see *Materials and Methods*) on the growth and morphology of the model filamentous fungus *A. nidulans*. In the absence of HSAF, germinating conidiospores displayed a normal pattern of morphogenesis that featured (Figures 1 and 2); i) an initial period of isotropic expansion, ii) emergence of a germ tube, and iii) hyphal extension along a stable polarity axis. By contrast, conidiospores germinated in the presence of HSAF (10–20 μg/ml) were typically unable to produce an obvious germ tube (Figure 1). For example, after 12 h in the presence of HSAF, only 3.5% of conidiospores possessed a germ tube that had extended a distance that was greater than the diameter of the swollen spore, compared with 99% of untreated controls (Figure 1). Indeed,

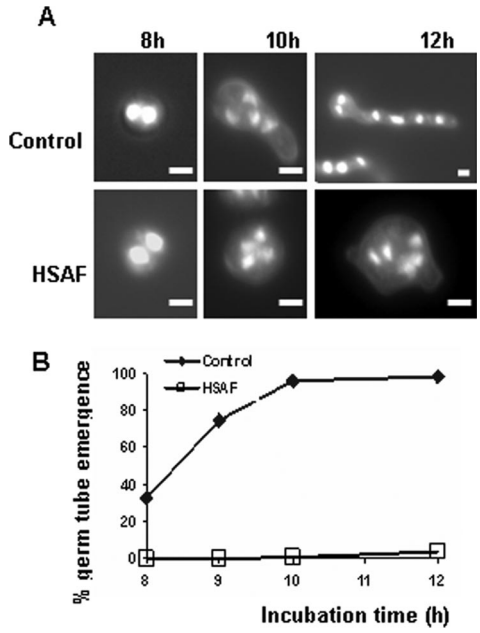

Figure 1. HSAF inhibits germ tube emergence. Conidia from wild-type strain A28 were germinated in YGV (A; top row) or YGV + 20 μg/ml HSAF (A; bottom row) for the indicated times and then stained with Hoechst 33258 and Calcofluor. Results from the time course are presented graphically in B. Bar, 3 μm.

many HSAF-treated spores featured small surface protuberances that could reflect failed attempts at forming a germ tube (Figure 1). Furthermore, when growing hyphae were exposed to similar concentrations of HSAF, hyphal extension ceased, tips swelled, and numerous branches formed at both apical and subapical sites (Figure 2). In addition, although nuclei appeared normal, they were often distributed as aberrant clumps (Figure 1). Identical morphological effects were observed when HPLC-purified HSAF was tested (S. Li *et al.*, unpublished results). These observations suggest that HSAF specifically targets processes required for the formation and maintenance of stable polarity axes, but does not affect growth or nuclear division.

Polarized hyphal growth is supported by the constant addition of new cell wall and membrane to a discrete apical site. In the presence of HSAF, this pattern was dramatically altered. Prominent patches of Calcofluor-bright cell wall material accumulated at the tips and apparent septation sites of treated hyphae (Figure 2, Calcofluor). Similar patches were never observed in untreated controls. In addition, within 10 min of exposure to HSAF, the normal apical localization of sterol-rich membrane microdomains was lost (Figure 2, filipin).

At hyphal tips, the *A. nidulans* formin SepA localizes to a broad cortical patch subtended by a bright spot (Sharpless and Harris, 2002; Figure 2, SepA-GFP). However, this localization pattern is rapidly disrupted (i.e., within 10 min) upon exposure to HSAF, and SepA accumulates within the cytoplasm (Figure 2, SepA-GFP). Longer treatment (i.e., 60 min) cause condensed SepA-GFP spots to appear at random locations throughout hyphae. The failure to maintain SepA at hyphal tips should preclude the formation of microfilaments that can be detected using a tropomyosin-GFP (TpmA-GFP) fusion protein (Pearson *et al.*, 2004). Thus, as expected, the disappearance of SepA from HSAF-treated hyphal tips was accompanied by loss of TpmA-GFP local-

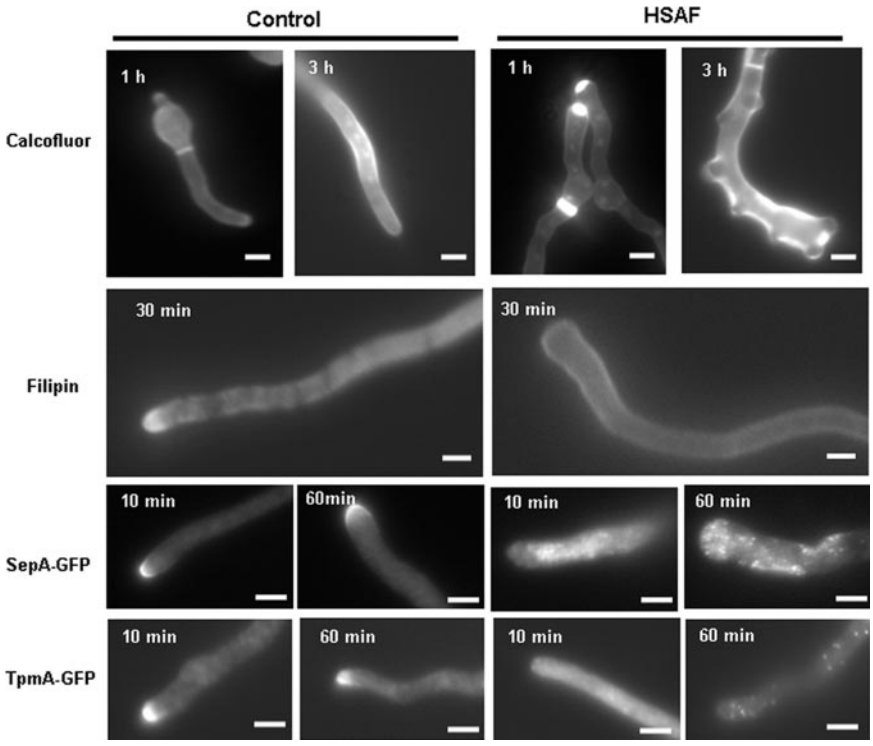

Figure 2. Morphological effects of HSAF on *A. nidulans*. Wild-type hyphae (strain A28) grown on YGV were shifted to YGV (control) or YGV + 20 μg/ml HASF for the indicated time. Cell walls and sterols were visualized by staining with Calcofluor and filipin, respectively. SepA was observed in hyphae expressing SepA-GFP (strain AKS70), and microfilaments were detected using TpmA-GFP (strain ACP115). Bar, 3 μm.

ization (Figure 2, TpmA-GFP). Together, these results imply that HSAF perturbs the stable recruitment of SepA to hyphal tips, thereby preventing the localized formation of microfilaments involved in vesicle transport. Notably, HSAF does not affect the localization of SepA or tropomyosin to septation sites, which is consistent with the observation that it has no affect on septum formation.

Mutation of an Acyl-CoA-dependent Ceramide Synthase Causes HSAF Resistance

To determine how HSAF affects polarized hyphal growth and to identify its presumptive target, a screen for mutants resistant to HSAF was undertaken. This screen yielded four *bar* (biocontrol agent resistance) mutants that were equally resistant to HSAF (both the partially purified methanol extracts and the HPLC-purified material; see *Materials and Methods* and Supplementary Figure 1). The *barA1* mutant, which was selected for further analysis, is resistant to HSAF and also exhibits a colony morphology defect at 42°C (Figure 3A). Note that the resistance phenotype appears to be specific to HSAF; *barA1* mutants retained wild-type susceptibility to aureobasidin A, myriocin, and nystatin (unpublished results). Genetic analysis revealed that resistance to the growth inhibitory effect of HSAF is dominant, whereas the colony and hyphal morphology defects are recessive. In addition, both traits cosegregated in backcrosses to wild type. The reduction in colony growth at 42°C was sufficient to permit cloning of the *barA* gene by complementation from a plasmid-borne genomic library (see *Materials and Methods* for details). The insert from a single rescued plasmid was positioned on the *A. nidulans* genome sequence (see *Materials and Methods*), and candidate open reading frames present on the insert were individually amplified and tested for complementation of *barA1*. These experiments revealed that *barA1* is a mutation in annotated open reading frame AN4332.2, which we now designate as *barA*. Complementation analysis showed that *barA* was the affected gene in the three other HSAF resistant mutants (*barA2, barA3, and barA4*). Sequencing of the four independent *barA* alleles demonstrated that *barA1*, *barA2*, and *barA3* possess different nonsense mutations (Supplementary Figure 2). These mutations would presumably lead to the formation of a nonfunctional truncated BarA protein, with the shortest consisting of only the first 161 amino acids. By contrast, *barA4* possesses a large (1576 base pairs) deletion that extends from 470 base pairs upstream to 1106-base pairs downstream of the predicted translational start site, thereby removing the entire coding region except for the last 377 base pairs. Because the growth defects and HSAF resistance caused by *barA4* are indistinguishable from the other *barA* mutations, these are all presumed to be null alleles.

BLAST searches revealed that BarA is a homologue of the yeast Lag1 acyl-CoA-dependent ceramide synthase (Table 2; Supplementary Figure 2), which catalyzes the condensation of phytosphingosine with a fatty acyl-CoA to form phytoceramide (Figure 3B). To determine if the *barA1* mutation causes morphological defects similar to those triggered by HSAF treatment, mutant hyphae were examined after growth at 42°C. These experiments showed no obvious delay in the emergence of germ tubes (Figure 4A). Nevertheless, once formed, *barA1* hyphae fail to maintain a stable axis of polarity, which results in extensive apical branching (Figure 4A; 58% of *barA1* mutants possess apical branches compared with 1% of wild-type hyphae; n = 100). Filipin staining at hyphal tips could not be detected in *barA1* mutants, nor could tropomyosin localization (Figure 4B). Notably, multiple attempts to transform *barA1* mutants with a SepA-GFP construct (Sharpless and Harris, 2002) were unsuccessful, thereby suggesting that the mutant could not tolerate increased dosage of SepA. In total, these phenotypes resemble those caused by HSAF treatment and are also similar to the defects observed after imposition of an downstream

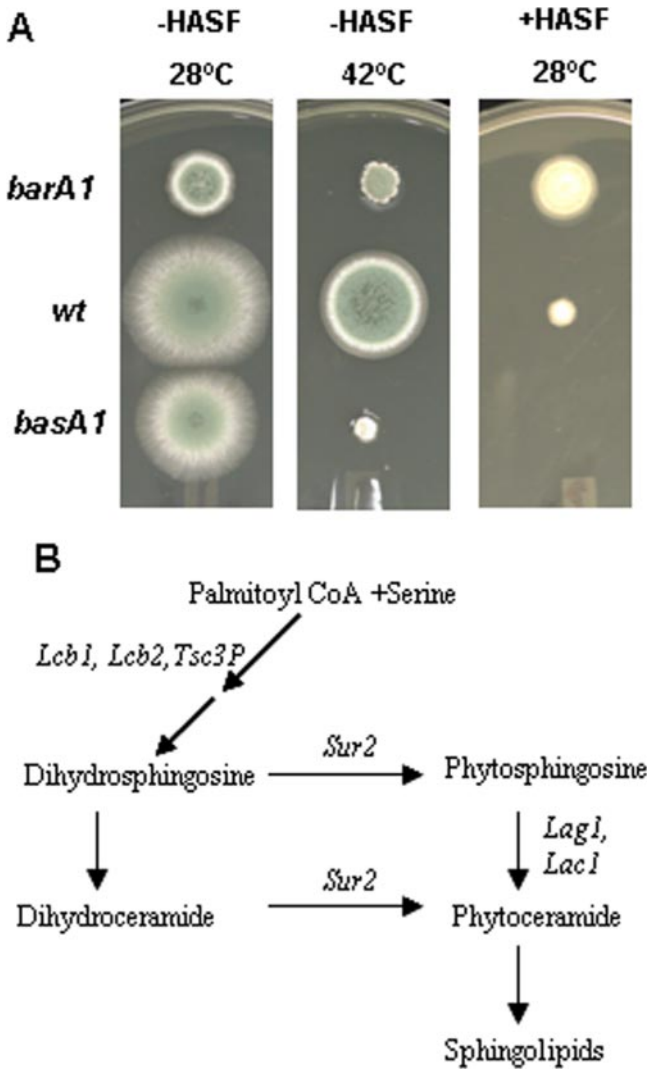

Figure 3. Mutants with altered responses to HSAF. (A) HSAF and temperature sensitivity of *barA1*, *basA1*, and wild-type strains. Conidia were inoculated onto MAG or MAG + 50 μg/ml HSAF plates and incubated at the indicated temperature for 3 d. (B) A simplified scheme of the Acyl-CoA-dependent sphingolipid synthesis pathway in yeast.

block in sphingolipid biosynthesis (Cheng *et al.*, 2001). Accordingly, we propose that the effects of HSAF require BarA-dependent ceramide synthesis. Although it is conceivable that BarA could be the target of HSAF, the observation that the morphological defects caused by the mutational inactivation of *barA* are not as severe as those caused by treatment of wild-type hyphae with HSAF (compare Figures 1 and 2 to Figure 4A) suggests that the role of BarA in HSAF resistance may not be direct (see *Discussion*).

Mutation of a Sur2 Homologue Causes HSAF Hypersensitivity

To further characterize the cellular response to HSAF, a large collection of Ts mutants was screened for mutations that cause hypersensitivity to HSAF at permissive temperature (28°C). Among several mutants identified, the one displaying the strongest hypersensitivity was named *basA* (biocontrol agent sensitivity; Figure 3A). Genetic analysis revealed that HSAF hypersensitivity and Ts growth were caused by a single recessive mutation. A single plasmid capable of complementing the Ts growth defect was recovered from a genomic library. The ends of the insert were sequenced, and testing of predicted coding regions for complementation demonstrated that *basA1* is a mutation in annotated open reading frame AN0640.2. Sequence analysis of the *basA1* allele showed that it is caused by a missense point mutation (TGG→TGC; W44C; Supplementary Figure 2). BLAST searches revealed that BasA is a homologue of the yeast Sur2 sphinganine hydroxylase (47% identity over 328 amino acids; Supplementary Figure 2). Notably, in yeast, the conversion of dihydrosphingosine (DHS) to phytosphingosine (PHS) by Sur2 generates one of the substrates for the Lag1 ceramide synthase (Figure 3B).

Table 2. BLASTp comparisons of *A. nidulans* and *S. cerevisiae* Lag1 homologues

Query	AN4332.2	AN2464.2	Lag1	Lac1
AN4332.2		29/49 $6e^{-24}$	31/38 $1e^{-22}$	29/47 $2e^{-21}$
BarA		277 aa	246 aa	221 aa
AN2464.2	30/51 $1e^{-22}$		51/67 $1e^{-86}$	43/58 $5e^{-84}$
LagA	230 aa		314 aa	379 aa

BarA and LagA were used as query sequences for BLASTp searches at NCBI using default paraemeters. For each entry, the top line includes the %identity/%similarity and the e value, and the botton line includes the length of predicted homology.

Phenotypic characterization of the *basA1* mutant revealed a striking similarity to the defects caused by HSAF in wild-type hyphae. Although there was no obvious delay in germ tube emergence, *basA1* mutants displayed extensive hyperbranching due to the apparent failure to maintain a stable axis of hyphal polarity (Figure 5A), as well as the loss of both filipin staining and tropomyosin localization at hyphal tips (Figure 5B). As noted for *barA1*, *basA1* mutants also appear sensitive to *sepA* gene dosage, as we could not recover transformants possessing SepA-GFP. Like HSAF-treated hyphae, *basA1* mutants display abnormal deposits of Calcofluor-stained cell wall material at random sites (Figure 5A). Separate experiments showed that this effect could be mimicked by the exposure of wild-type hyphae to increased levels of DHS (1 μg/ml), which is predicted to accumulate in *basA1* mutants (Figure 3B), whereas the addition of PHS (0.5–1 μg/ml) had no comparable effect (unpublished results). Collectively, these experiments suggest that the effects of HSAF on hyphal morphogenesis and cell wall deposition are exacerbated by the depletion of PHS, a ceramide precursor, and perhaps also the accumulation of DHS.

A. nidulans Possesses Two Distinct Ceramide Synthases

Simultaneous deletion of the two closely related acyl-CoA-dependent ceramide synthases in S. cerevisiae, Lag1 and Lac1, severely compromises growth (Barz and Walter, 1999; Schorling *et al.*, 2001). By contrast, *barA* mutants are able to grow, albeit with abnormal hyphal morphology. This suggests that *A. nidulans* possesses a second ceramide synthase. Searches of the *A. nidulans* genome database identified another annotated coding region, AN2464.2, with much stronger predicted homology to the yeast Lag1 ceramide synthases than that displayed by BarA (Table 2; Supplementary Figure 2). Phylogenetic analysis (Figure 6) confirmed that this homologue belongs to a distinct clade that includes *S.*

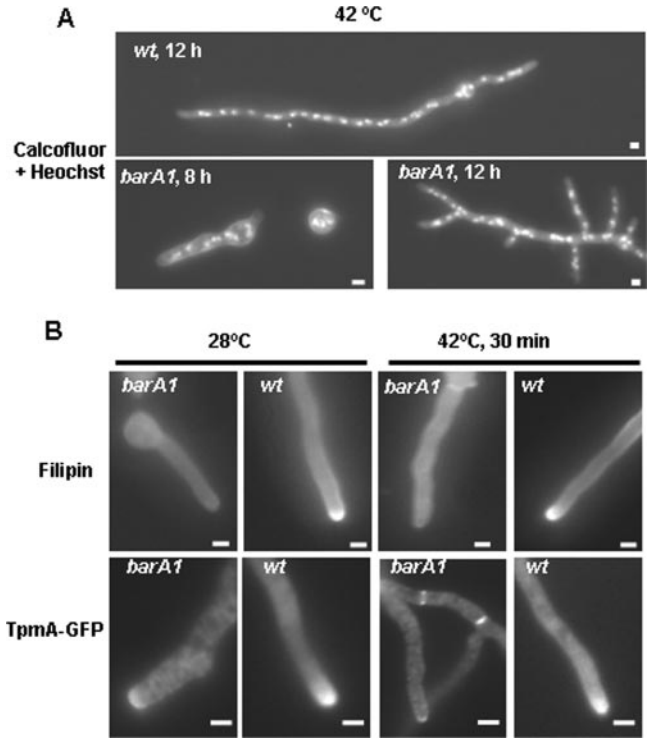

Figure 4. Functional characterization of BarA. (A) Wild-type (wt) and *barA 1* conidia were germinated in YGV at 42°C for 8 or 12 h and then stained with Hoechst 33258 and Calcofluor. (B) Wild-type and *barA1* hyphae grown in YGV were shifted to fresh YGV at either 28° or 42°C. After 30 min, hyphae were stained with filipin to observe sterols. Microfilaments were detected in wild-type and *barA1* hyphae expressing TpmA-GFP. Bar, 3 μm.

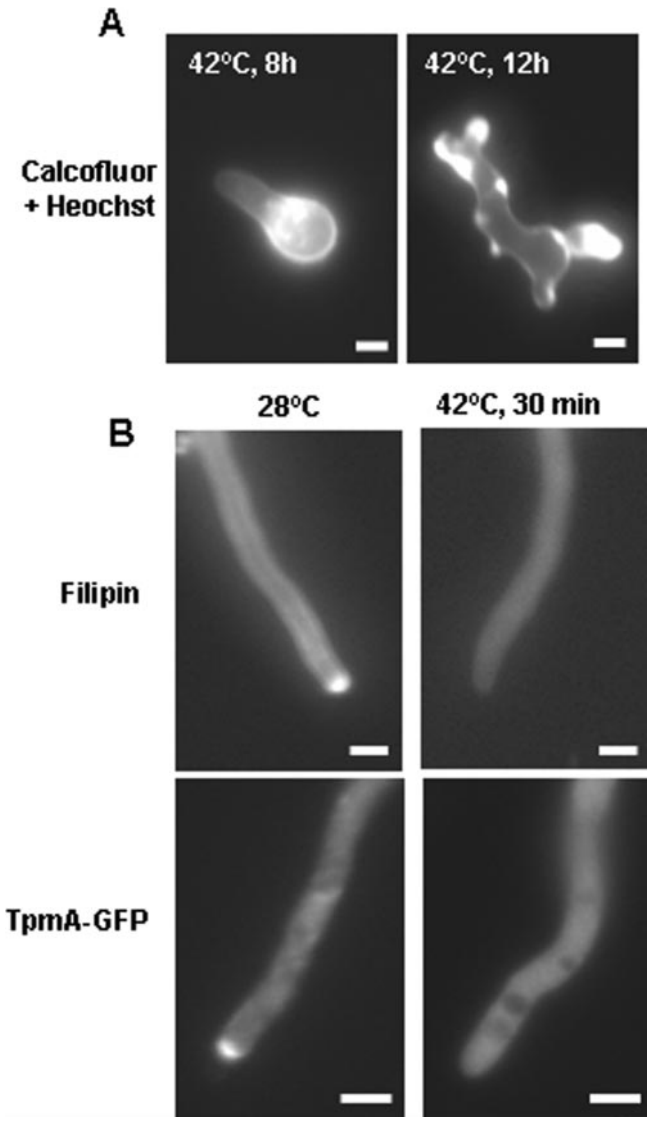

Figure 5. Functional characterization of BasA. (A) *basA1* conidia were germinated in YGV at 42°C for 8 or 12 h and then stained with Heochst 33258 and Calcofluor. (B) *basA1* hyphae were shifted into fresh YGV medium and incubated at 28 or 42°C for 30 min. Sterols were visualized by staining with filipin. Microfilaments were detected by localizing TpmA-GFP. Bar, 3 μm.

cerevisiae Lag1 and Lac1, plus single homologues from other filamentous fungi and yeasts. Accordingly, we named this homologue LagA. Notably (Figure 6), BarA belongs to a separate clade that consists of members from other filamentous fungi and *Schizosaccharomyces pombe*, but not *S. cerevisiae*. On the basis of this analysis, we sought to determine if LagA is an essential ceramide synthase in *A. nidulans*.

A precise replacement of *lagA* was constructed (Δ*lagA*::*pyr-4*), but could only be propagated as a heterokaryon. Homokaryotic segregants produced morphologically abnormal hyphae with a severe growth defect (Supplementary Figure 4), thereby suggesting that *lagA* is an essential gene. To further characterize its function, we generated a conditional allele regulated by the *alcA* promoter (*alcA*(p)::*GFP*::*lagA*; see *Materials and Methods*). When grown under inducing conditions, this strain grew as well as wild-type controls and displayed normal colony morphology (Figure 7A). However, on repressing media, the *alcA*(p)::*lagA* strain grew much worse than the wild-type or the *barA1* mutant (compared with wild type, radial growth of *alcA*(p)::*lagA* was reduced by 91%, whereas *barA1* was reduced by only 63%; Figure 7A). Although germ tube emergence was unaffected, repressed *alcA*(p)::*lagA* hyphae ultimately became grossly distorted with multiple apical branches and no obvious polarity axis (Figure 8A). Nevertheless, unlike *barA1* mutants, the growth and morphological defects caused by repression of *lagA* expression were further exacerbated by exposure to HSAF (Figure 7B). Finally, we constructed and characterized a *barA1 alcA*(p)::*lagA* double mutant. Although this mutant was indistinguishable from *barA1* when *alcA*(p) was induced, it displayed a severe growth defect on repressing media (Figure 8C). Under the latter conditions, double mutant conidiospores were only capable of producing short, morphologically aberrant hyphae (Figure 8, A and B). Based on this synthetic morphological defect, we conclude that LagA and BarA both have significant roles in hyphal morphogenesis. In particular, we propose that LagA is an essential ceramide synthase that generates the bulk of ceramide pools required for the polarized growth of *A. nidulans* hyphae. By contrast, BarA appears produce a specialized pool that is particularly important for organization of the hyphal tip and is presumably targeted by HSAF.

Depletion of Sphingolipids in barA and lagA Mutants

To further characterize the roles of BarA and LagA in ceramide synthesis, we used labeled DHS to examine de novo

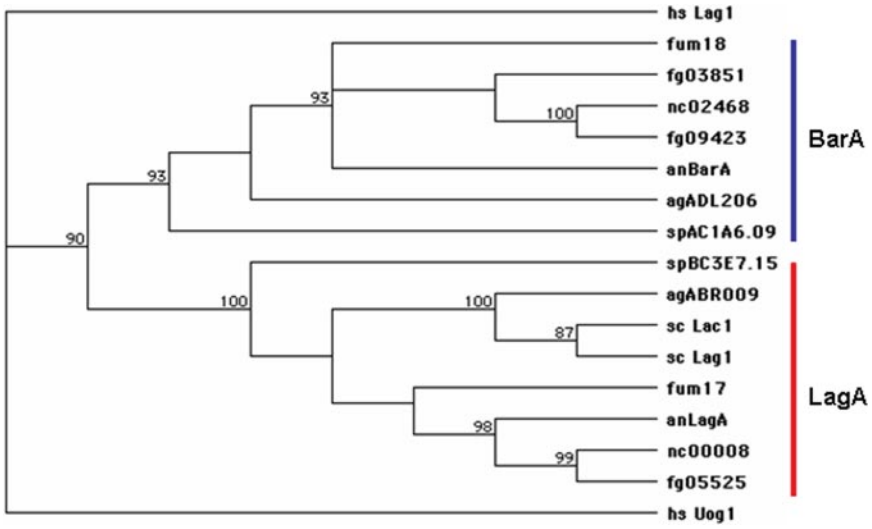

Figure 6. Fungal Lag1-related acyl-CoA-dependent ceramide synthases. Predicted coding regions of Lag1 homologues were aligned using ClustalW (MacVector v7.0). The tree was constructed using the neighbor joining method with bootstrap support (1000 repetitions) and Poisson correction. All sequences are designated according to their annotation format or known protein name. *A. nidulans* (An), *N. crassa* (Nc), and *F. graminearum* (Fg) sequences were obtained from the Fungal Genome Initiative (http://www.broad.mit.edu/annotation/fungi/fgi/). *F. verticillioides* (Fum17 and Fum18), *S. pombe* (Sp), *Ashbya gossypii*, (Ag), *S. cerevisiae* (Sc), and human (Hs) sequences were obtained from NCBI. The blue line indicates BarA homologues, and the red line indicates LagA homologues.

sphingolipid biosynthesis in wild-type, *barA1*, *alcA*(p)::*lagA*, and *barA1 alcA*(p)::*lagA* strains. Although wild-type lipid extracts possessed two prominent bands of labeled sphingolipids, sphingolipid levels were dramatically reduced in extracts from either single mutant or the double mutant (Figure 9). Moreover, PHS accumulated in the *barA1* mutant, and to a lesser extent in the *alcA*(p)::*lagA* strain (Figure 9). Surprisingly, PHS accumulation was not observed in the double mutant. Collectively, these results suggest that BarA and LagA are bona fide ceramide synthases and support the notion that the morphological defects caused by their mutational inactivation is due to the depletion of ceramide pools.

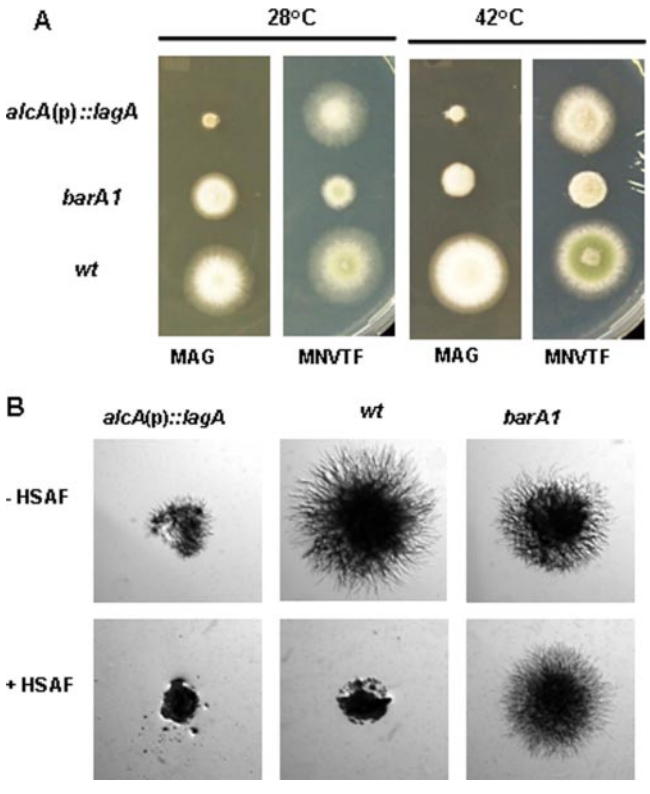

Figure 7. Functional characterization of LagA. (A) Comparison of growth defects observed in *barA1* and *lagA108* mutants. Conidiospores from strains ASL10 (*alcA*(p)*::lagA*), UV13 (*barA1*) and A28 (wild type) were inoculated on *alcA*(p)-inducing (MNVTF) or -repressing (MAG) media and incubated at the indicated temperatures for 3 d. (B) The *alcA*(p)::*lagA* mutant is sensitive to HSAF. Conidiospores with the indicated genotypes were inoculated onto MAG + 50 μg/ml HSAF plates and incubated for 24 h. Images were acquired using an Olympus SZX12 dissecting microscope (Lake Success, NY).

DISCUSSION

It has become increasingly apparent that the formation of a stable polarity axis is a key event underlying hyphal mor-

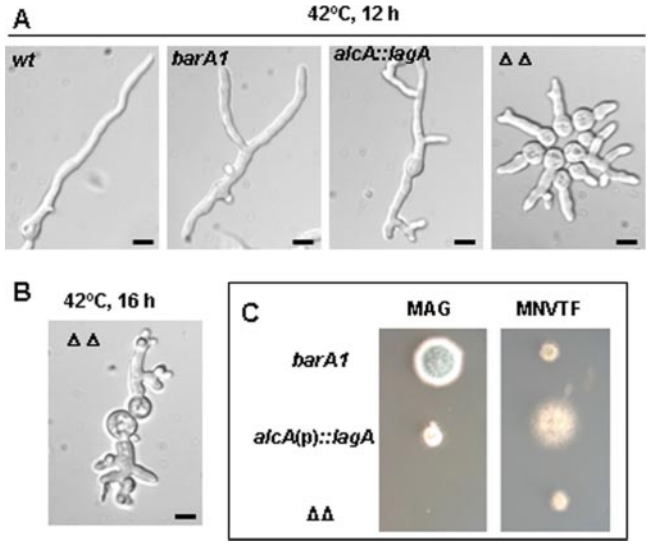

Figure 8. Phenotype of *barA lagA* double mutants. (A and B) Wild-type (A28), *barA1* (UV13), *alcA*(p)::*GFP*::*lagA* (ASL10), and *barA1 alcA*(p)::*GFP*::*lagA* (DRG1; ΔΔ) conidia were germinated in *alcA*(p) repressing YGV at 42°C for 12 (A) or 16 h (E). (C) Conidiospores from strains UV13, ASL10, and DRG1 were inoculated on *alcA*(p)-inducing (MNVTF) or -repressing (MAG) media and incubated at 28°C for 3 d. Bar, 10 μm.

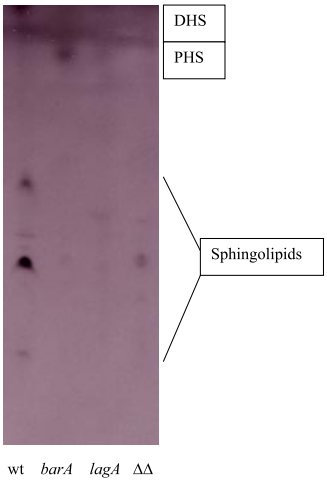

Figure 9. Sphingolipid levels are reduced in *barA* and *lagA* mutants. The de novo biosynthesis of sphingolipids was examined in hyphae labeled with [4,5-[^{3}H]DHS. Lipids were extracted and analyzed by TLC as described in the *Materials and Methods*. The following strains were used; GR5 (wt), UV13 (*barA1*), ASL10 (*alcA*(p)::*lagA*), and DRG1 (ΔΔ). The migration of sphingolipids, PHS, and DHS is based on known standards.

phogenesis (Harris and Momany, 2004). Recent studies highlight the role of conserved signaling modules and novel fungal-specific proteins in controlling this event (Bauer *et al.*, 2004; Pearson *et al.*, 2004). Here, we exploit a small molecule that perturbs the normal pattern of hyphal morphogenesis to demonstrate that the formation and stabilization of polarity axes requires functional ceramide synthases. Moreover, we show that filamentous fungi possess two distinct acyl-CoA-dependent ceramide synthases, one that is essential and a second that appears to be uniquely dedicated to the regulation of polarized hyphal growth.

Plasma membrane microdomains are generally thought to serve as localized signaling platforms that facilitate the transduction of cell surface information to the cytoskeleton. These segregated microdomains, also known as lipid rafts, form in the lateral plane of the membrane and are composed of sphingolipids and sterols (Simons and Toomre, 2000; Tsui-Pierchala *et al.*, 2002). Although there is some controversy regarding their existence (Munro, 2003), it has become increasingly apparent that plasma membrane microdomains play an important role in the regulation of polarized morphogenesis. For example, in neurons, lipid rafts have been implicated in the regulation of growth cone guidance by chemotropic signals (Guirland *et al.*, 2004). More recently, distinct receptor-ligand complexes were shown to segregate into different membrane microdomains on the same axonal growth cone (Marquardt *et al.*, 2005). This result is consistent with the idea that a diverse array of lipid microdomains may exist on the surface of a single polarized cell. The basis for this diversity may lie in the sphingolipid composition of each microdomain. The observation that different microdomains on the neuronal cell surface contain distinct sphingolipids that are presumably derived from separate ceramide pools supports this notion (Brugger *et al.*, 2004). Indeed, it has been demonstrated that mammalian cells possess multiple Lag1 homologues that differ in the nature and length of the fatty acyl-CoA donor (Riebeling *et al.*, 2003). On the basis of our results, we propose that a similar complexity in organization and composition of plasma membrane microdomains underlies the regulation of polarized hyphal growth.

In *S. cerevisiae*, the acyl-CoA-dependent ceramide synthases Lag1 and Lac1 form a complex with an additional subunit known as Lip1 (Vallee and Riezman, 2005). Within this complex, the synthases may associate with each other as heterodimers or with themselves as homodimers. Characterization of Lip1 shows that it is essential for ceramide synthase activity and, along with Lag1 and Lac1, localizes to the ER membrane (Vallee and Riezman, 2005). Although the specific function of Lip1 remains uncertain, it has been suggested that Lag1 and Lac1 may regulate the specificity of the fatty acyl-CoA donor (Guillas *et al.*, 2001). Our results imply that, like yeast, filamentous fungi possess an essential Lag1 homologue that presumably generates most of the ceramide required for growth and hyphal morphogenesis. However, they also possess a distinct homologue that is absent from yeast and appears to be dedicated to the regulation of polarized hyphal growth. On the basis of our characterization of *barA* mutants and the effects of HSAF, we propose that this homologue uses an alternate acyl-CoA donor to generate a specific pool of sphingolipids that are incorporated into a lipid microdomain at the hyphal tip. This hypothesis predicts the existence of two different ceramide synthase complexes in filamentous fungi. Annotation of the genome sequences of multiple filamentous fungi (i.e., *A. nidulans*, *Neurospora crassa*, *Fusarium graminearum*, *Magnaporthe grisea*) has failed to reveal obvious homologues of Lip1. Therefore, at this time, determining the biochemical composition of these complexes and the nature of their donor specificity is an important target for future research.

In filamentous fungi, the formation and maintenance of a stable polarity axis is essential for polarized hyphal growth. Functions known to be required for axis stabilization include the Bud1 GTPase signaling module and kinesin-based microtubule transport (Bauer *et al.*, 2004; Konzack *et al.*, 2005). Several previous observations also implicate membrane microdomains in this process. First, lipid rafts appear to be required for polarized hyphal growth in *Candida albicans* and mating projection formation in yeast (Bagnat and Simons, 2002; Martin and Konopka, 2004; though see Valdez-Taubus and Pelham, 2003 for an alternative interpretation of the yeast results). Second, an earlier study in *A. nidulans* documented a role for sphingolipid-rich membrane microdomains in the regulation of polarized hyphal growth (Cheng *et al.*, 2001). Third, we recently described a novel fungal-specific protein required for axis stabilization that appears to regulate membrane organization at the hyphal tip (Pearson *et al.*, 2004). Our results extend these previous observations by showing that filamentous fungi possess a unique acyl-CoA-dependent ceramide synthase that appears to promote the formation of a specialized membrane microdomain required to stabilize polarity axes. Moreover, the presence of distinct Lag1-related ceramide synthases that make independent contributions to polarized hyphal growth suggests the possible existence of distinct membrane microdomains at the hyphal tip. How could these lipid microdomains mediate the stabilization of polarity axes? One attractive possibility is that they provide anchoring regions for morphogenetic scaffold proteins such as formins and WASP, thereby placing these proteins in proximity to the upstream GTPases that trigger their activation (Evangelista *et al.*, 1997; Golub and Caroni, 2005). For instance, a BarA-dependent microdomain may regulate the localization of SepA, whereas the function of WASP and other crucial morphogenetic proteins may require a parallel LagA-dependent microdomain (Figure 10). Moreover, the presence of the LagA-

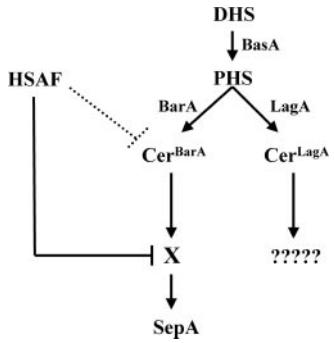

Figure 10. Schematic representation of ceramide synthesis pathways in *A. nidulans*. BarA and LagA are proposed to direct the synthesis of distinct ceramide pools that independently regulate polarized hyphal growth. Through "X," the hypothetical target of HSAF, BarA-dependent ceramides are implicated in the localization of SepA. The morphogenetic functions affected by the LagA-dependent pool remain unknown (see text for details). The dashed line indicates the possibility that HSAF could directly target BarA.

dependent microdomain may be sufficient to sustain polarized hyphal growth when BarA function is eliminated, thereby accounting for the synthetic defects observed in the *barA1 alcA*(p)::*lagA* double mutant.

Our results demonstrate that HSAF, an antifungal polyketide produced by the bacterial biocontrol agent *Lysobacter enzymogenes* C3, disrupts the formation of stable polarity axes by affecting formin-mediated microfilament assembly at hyphal tips. Furthermore, the cellular response to HSAF requires an intact ceramide biosynthetic pathway. In particular, mutations affecting the BarA ceramide synthase confer HSAF resistance, whereas a mutation in the BasA sphinganine hydroxylase causes hypersensitivity. One interpretation of our results is that HSAF directly targets BarA, thereby causing depletion of a specific ceramide pool that is important for polarized growth (Figure 10; dotted line). However, if this were true, the morphological defects caused by null mutations in *barA* should essentially be the same as those triggered by the treatment of wild-type hyphae with HSAF. Because this is clearly not the case, we favor an alternative interpretation whereby the localization of the bona fide HSAF target is dependent on a ceramide pool generated by BarA (Figure 10). For example, the effects of HSAF may require that its target (i.e., X in Figure 10) be properly localized within a BarA-dependent plasma membrane microdomain. The dispersal of "X" in *barA* mutants may have several consequences. These may include reducing its affinity for HSAF while only modestly affecting its function, or, altering the interaction with HSAF such that it leads to the abnormal activation of a compensatory pathway. Note that the latter possibility could explain the dominance of the HSAF-resistance phenotype in *barA* mutants. Finally, by inactivating the parallel LagA pathway that sustains polarized growth when BarA-dependent functions are compromised (Figure 10), the *basA1* mutation could conceivably cause HSAF hypersensitivity.

In summary, we have identified a novel antifungal compound that perturbs hyphal morphogenesis. We have exploited this compound to discover an acyl-CoA-dependent ceramide synthase that is unique to filamentous fungi and is required for the formation of a stable axis of hyphal polarity. Our results suggest that further study of this specialized sphingolipid biosynthetic pathway will provide important insights into its role in the regulation of polarized hyphal growth.

ACKNOWLEDGMENTS

We thank the anonymous reviewers for their thoughtful suggestions. This study was supported by an award from the Nebraska Research Initiative.

REFERENCES

Bagnat, M., and Simons, K. (2002). Cell surface polarization during yeast mating. Proc. Natl. Acad. Sci. USA *99*, 14183–14188.

Bartnicki-Garcia, S. (2002). Hyphal tip growth: outstanding questions. In: Molecular Biology of Fungal Development, ed. H. D. Osiewacz, New York: Marcel Dekker, 29–58.

Bartnicki-Garcia, S., and Lippman, E. (1969). Fungal morphogenesis: cell wall construction in *Mucor rouxii*. Science *165*, 302–304.

Barz, W. P., and Walter, P. (1999). Two endoplasmic reticulum (ER) membrane proteins that facilitate ER-to-Golgi transport of glycosylphosphatidylinositol-anchored proteins. Mol. Biol. Cell *10*, 1043–1059.

Bauer, Y., Knechtle, P., Wendland, J., Helfer, H., and Philippsen, P. (2004). A Ras-like GTPase is involved in hyphal growth guidance in the filamentous fungus *Ashbya gossypii*. Mol. Biol. Cell *15*, 4622–4632.

Brugger, B., Graham, C., Leibrecht, I., Mombelli, E., Jen, A., Wieland, F., and Morris, R. (2004). The membrane domains occupied by glycosylphosphatidylinositol-anchored prion protein and Thy-1 differ in lipid composition. J. Biol. Chem. *279*, 7530–7536.

Cheng, J., Park, T. S., Fischl, A. S., and Ye, X. S. (2001). Cell cycle progression and cell polarity require sphingolipid biosynthesis in *Aspergillus nidulans*. Mol. Cell. Biol. *21*, 6198–6209.

Efimov, V. P. (2003). Roles of NUDE and NUDF proteins of *Aspergillus nidulans*: insights from intracellular localization and overexpression effects. Mol. Biol. Cell *14*, 871–888.

Efimov, V. P., and Morris, N. R. (1998). A screen for dynein synthetic lethals in *Aspergillus nidulans* identifies spindle assembly checkpoint genes and other genes involved in mitosis. Genetics *149*, 101–116.

Evangelista, M., Blundell, K., Longtine, M. S., Chow, C. J., Adames, N., Pringle, J. R., Peter, M., and Boone, C. (1997). Bni1p, a yeast formin linking Cdc42p and the actin cytoskeleton during polarized morphogenesis. Science *276*, 118–122.

Futerman, A., and Hannun, Y. A. (2004). The complex life of simple sphingolipids. EMBO Rep. *5*, 777–782.

Golub, T., and Caroni, P. (2005). PI(4,5)P2-dependent microdomain assemblies capture microtubules to promote and control leading edge motility. J. Cell Biol. *169*, 151–165.

Gooday, G. W. (1971). An autoradiographic study of hyphal growth of some fungi. J. Gen. Microbiol. *67*, 125–133.

Graupner, P. R., Thornburgh, S., Mathieson, J. T., Chapin, E. L., Kemmitt, G. M., Brown, J. M., and Snipes, C. E. (1997). Dihydromaltophilin; a novel fungicidal tetrameric acid containing metabolite from *Streptomyces* sp. J. Antibiot. *50*, 1014–1019.

Guillas, I., Kirchman, P. A., Chuard, R., Pfefferli, M., Jiang, J. C., Jazwinski, S. M., and Conzelmann, A. (2001). C26-CoA-dependent ceramide synthesis of *Saccharomyces cerevisiae* is operated by Lag1p and Lac1p. EMBO J. *20*, 2655–2665.

Guirland, C., Suzuki, S., Kojima, M., Lu, B., and Zheng, J. Q. (2004). Lipid rafts mediate chemotropic guidance of nerve growth cones. Neuron *42*, 51–62.

Harris, S. D. (2001). Genetic analysis of ascomycete fungi. In: Molecular and Cellular Biology of Filamentous Fungi: Practical Approach, ed. N. Talbot, Oxford: Oxford University Press, 47–58.

Harris, S. D., and Momany, M. (2004). Polarity in filamentous fungi: moving beyond the yeast paradigm. Fungal Genet. Biol. *41*, 391–400.

Harris, S. D., Morrell, J. L., and Hamer, J. E. (1994). Identification and characterization of *Aspergillus nidulans* mutants defective in cytokinesis. Genetics *136*, 517–532.

Harris, S. D., Hamer, L., Sharpless, K. E., and Hamer, J. E. (1997). The *Aspergillus nidulans sepA* gene encodes an FH1/2 protein involved in cytokinesis and the maintenance of cellular polarity. EMBO J. *16*, 3474–3483.

Harris, S. D., Read, N. D., Roberson, R. W., Shaw, B., Seiler, S., Plamann, M., and Momany, M. (2005). Polarisome meets Spitzenkorper: microscopy, genetics, and genomics converge. Euk. Cell *4*, 225–229.

Higgs, H. N., and Peterson, K. J. (2005). Phylogenetic analysis of the formin homology 2 domain. Mol. Biol. Cell *16*, 1–13.

Jakobi, M., Winkelmann, G., Kaiser, D., Kempler, C., Jung, G., Berg, G., and Bahl, H. (1996). Maltophilin: a new antifungal compound produced by *Stenotrophomonas maltophila* R3089. J. Antibiot. *49*, 1101–1104.

Kafer, E. (1977). Meiotic and mitotic recombination in *Aspergillus* and its chromosomal aberrations. Adv. Genet. *19*, 33–131.

Konzack, S., Rischitor, P. E., Enke, C., and Fischer, R. (2005). The role of the kinesin motor KipA in microtubule organization and polarized growth of *Aspergillus nidulans*. Mol. Biol. Cell *16*, 497–506.

Li, S. (2005). An antifungal metabolite from *Lysobacter enzymogenes* strain C3, isolation, biological activity, mode of action and potential use in plant disease control. PhD thesis. University of Nebraska-Lincoln.

Marquardt, T., Shirasaki, R., Ghosh, S., Andrews, S. E., Carter, N., Hunter, T., and Pfaff, S. L. (2005). Coexpressed EphA receptors and ephrin-A ligands mediate opposing actions on growth cone navigation from distinct membrane domains. Cell *121*, 127–139.

Martin, S., and Konopka, J. B. (2004). Lipid raft polarization contributes to hyphal growth in *Candida albicans*. Euk. Cell *3*, 675–684.

Merrill, A. H., Jr. (2002). De novo sphingolipid biosynthesis: a necessary, but dangerous, pathway. J. Biol. Chem. *277*, 25843–25846.

Munro, S. (2003). Lipid rafts: elusive or illusive. Cell *115*, 377–388.

Oakley, B. R., and Osmani, S. A. (1993). Cell cycle analysis using the filamentous fungus *Aspergillus nidulans*. In: The Cell Cycle: Practical Approach, ed. P. Fantes, R. Brooks, Oxford: Oxford University Press, 127–142.

O'Connell, M. J., Osmani, A. H., Morris, N. R., and Osmani, S. A. (1992). An extra copy of $nimE^{cyclinB}$ elevates pre-MPF levels and partially suppresses mutation of $nimT^{cdc25}$ in *Aspergillus nidulans*. EMBO J. *11*, 2139–2149.

Osherov, N., and May, G. (2000). Conidial germination in *Aspergillus nidulans* requires RAS signaling and protein synthesis. Genetics *155*, 647–656.

Pearson, C. L., Xu, K., Sharpless, K. E., and Harris, S. D. (2004). MesA, a novel fungal protein required for the stabilization of polarity axes in *Aspergillus nidulans*. Mol. Biol. Cell *15*, 3658–3672.

Riebeling, C., Allegood, J. C., Wang, E., Merrill, A. H., Jr., and Futerman, A. H. (2003). Two mammalian longevity assurance gene (LAG1) family members, trh1 and trh4, regulate dihydroceramide synthesis using different fatty acyl-CoA donors. J. Biol. Chem. *278*, 43452–43459.

Sagot, I., Klee, S. K., and Pellman, D. (2002). Yeast formins regulate cell polarity by controlling the assembly of actin cables. Nat. Cell. Biol. *4*, 42–50.

Schorling, S., Vallee, B., Barz, W. P., Riezman, H., and Oesterhelt, D. (2001). Lag1p and Lac1p are essential for the Acyl-CoA-dependent ceramide synthase reaction in *Saccharomyces cerevisiae*. Mol. Biol. Cell *12*, 3417–3427.

Sharpless, K. E., and Harris, S. D. (2002). Functional characterization and localization of the *Aspergillus nidulans* formin SEPA. Mol. Biol. Cell *13*, 469–479.

Sheu, Y. J., Santos, B., Fortin, N., Costigan, C., and Snyder, M. (1998). Spa2p interacts with cell polarity proteins and signaling components involved in yeast cell morphogenesis. Mol. Cell. Biol. *18*, 4053–4069.

Simons, K., and Toomre, D. (2000). Lipid rafts and signal transduction. Nat. Rev. Mol. Cell Biol. *1*, 31–39.

Tsui-Pierchala, B. A., Encinas, M., Milbrandt, J., and Johnson, E. M., Jr. (2002). Lipid rafts in neuronal signaling and function. Trends Neurosci. *25*, 412–417.

Valdez-Taubus, J., and Pelham, H. R. (2003). Slow diffusion of proteins in the yeast plasma membrane allows polarity to be maintained by endocytic cycling. Curr. Biol. *13*, 1636–1640.

Vallee, B., and Riezman, H. (2005). Lip1, a novel subunit of acyl-CoA ceramide synthase. EMBO J. *24*, 730–741.

Yang, L., Ukil, L., Osmani, A., Nahm, F., Davies, J., De Souza, C. P., Dou, X., Perez-Balaguer, A., and Osmani, S. A. (2004). Rapid production of gene replacement constructs and generation of a green fluorescent protein-tagged centromeric marker in *Aspergillus nidulans*. Euk. Cell *3*, 1359–1362.

Yuen, G., Steadman, J. R., Lindegren, D. T., Schaff, D., and Jochum, C. (2001). Bean rust biological control using bacterial agents. Crop. Protect. *20*, 395–402.

Zhang, Z., and Yuen, G. Y. (1999). Biological control of *Bipolaris sorokiniana* on tall fescue by *Stenotrophomonas maltophilia* strain C3. Phytopathology *89*, 817–822.